3D - CFD Heat Transfer Simulation within Spark Ignition Engine

محاكاة عددية ثلاثية الأبعاد لانتقال الحرارة في محرك أحتراق بالشرارة

Assist. Prof. Dr. Mahmoud. A. Mashkour[1] MahmoodMashkoor@hotmail.com
M.Sc. Student Mustafa Hadi Ibraheem[2] abc_logo@yahoo.com
Mechanical Engineering Department/U.O.T

Abstract

Heat transfer influence largely engine performance and reliability of thermo- mechanical of engine components. As a consequence, an accurate prediction of the wall heat fluxes of the combustion chamber walls is crucial and complex, as a result for the complexity of the phenomena that occurs in the mechanism of heat transfer within combustion chamber. The simulation fulfillment was achieved using a gasoline fueled engine. 3D-CFD was executed utilizing dynamic mesh technique using ANSYS with respect to the crank angles for the four – stroke ignition engine at difference engine speeds (1500, 2000, 2500 rpm). The aim of this context is to estimate the flow characteristics and heat transfer coefficient of in – cylinder and exhaust manifold for SI engine. The results of the simulation were compared and were validated with other published.

Keywords: Heat transfer, 3D-CFD, Dynamic mesh technique, SI engine, exhaust manifold.

الخلاصة

يؤثر نقل الحرارة بشكل كبير على أداء المحرك وموثوقية المكونات الميكانيكية الحرارية للمحركات. ونتيجة لذلك ، فإن التنبؤ الدقيق لتدفق الحرارة لجدران غرفة الاحتراق أمر بالغ الأهمية ومعقد ، نتيجة لتعقيد الظواهر التي تحدث في آلية نقل الحرارة داخل غرفة الاحتراق. تم إنجاز المحاكاة باستخدام محرك يعمل بالبنزين. تم تنفيذ 3D-CFD باستخدام تقنية شبكة ديناميكية باستخدام ANSYS فيما يتعلق بزوايا الكرنك لمحرك الإشعال رباعي الأشواط عند سرعات محرك مختلفة (1500 ، 2000 ، 2500 دورة في الدقيقة). والهدف من هذا البحث هو تقدير خصائص التدفق ومعامل نقل الحرارة في غرفة الاحتراق ومجمع العادم لمحرك SI. وتمت مقارنة نتائج المحاكاة وتم التحقق من صحتها مع غيرها من المنشورات.

الكلمات المفتاحية : أنتقال الحرارة، تحليل عددي ثلاثي الأبعاد، تقنية الشبكة الديناميكية، محرك أشتعال بالشرر، مجمع العادم.

Nomenclature

SI	Spark Ignition Engine
rpm	Revolution per Minutes
CA	Crank angle
TDC	Top Dead Center
BDC	Bottom Dead Center
ATDC	After Top Dead Center
BTDC	Before Top Dead Center
θ_c	Current crank angle (deg.)
θ_s	Start angle (deg.)
t	Time (sec.)
Ω	Shaft speed (rpm)
θ event	Event crank angle
n	Integer
θ_{period}	Crank angle period (sec.)
P_s	Piston Position
A	Piston Stroke (mm)
L	Connecting Rod Length (mm)
ρ	Total mass density (kg m^{-3})
u	Velocity (m/sec.)
τ	Stress tensor (N/m^2)
φ	Viscous dissipation function
S	Source term
P	Pressure (Pa)
k	Thermal conductivity (W/m.k)
h	Heat transfer coefficient ($W/m^2.k$)

Introduction

One of the considerable factors which control the air-fuel mixing and combustion process, also have a significant important on heat transfer is a motion of fluid inside the engine. The modeling of flow and heat transfer in the internal combustion engine (ICE) represents one of the highest level of complexity and a challenging task. This is because the variety of fluid properties due to unsteady state during engine cycle. Therefore, the study and development the fluid flow and heat transfer process in the internal combustion engines required to characterize deeply what happens from the complex physical phenomenon within engine. Heat transfer on the wall of a combustion chamber plays a major function on the behavior of the material of wall, thermal efficiency of engine, life of the component of engines also, the emissions of NO_x, unburned hydrocarbon, knock and their action rely on the temperature of the in – cylinder gases. Thus, the characterization of thermal energy, heat transfer rate, and heat rate release has become a key focus in recent time. James and Alexandros 1978 [1] investigated the effect of the temperature of the combustion chamber surface on the emissions of exhaust was inspected for wide ranges of air to fuel ratio, the speed of engine for a 6.5 L V8. The research presents that the emissions of NO_x significantly increase with increasing the temperature of surface. Alkidas 1982 [2] recorded the magnitude of the instantaneous heat flux on the cylinder head for 830 cm^3 four – stroke (SI) engine, deduced that it could be influenced by the speed of the engine, volumetric efficiency, and air to fuel ratio. Heywood 1988 [3] presented a brief survey of heat transfer of engine, the correlations and results are summarized from various studies of different heat transfer mechanism, average, spatially, and instantaneous local heat transfer and the influence of every one on the performance of engine. Harigaya et al. 1993 [4] evaluated instantaneous local heat transfer coefficient on the surface of combustion chambers for three types. The influence of flame propagation and flow gases on the heat transfer coefficient was investigated. The paper deduced a relation between the heat transfer coefficient and velocity of flame at different location. Kleemann et al. 2001 [5] utilizing CFD package, estimated the heat transfer in diesel engines that operating at high peak pressure where, precise estimations of thermal of the material components are required. Mohammadi el at. 2008 [6] scrutinized the heat transfer coefficient, heat flux, on the wall of cylinder, the cylinder head, and piston. The paper proposed a new correlation to estimate the minimum and the maximum heat transfer coefficient within the combustion chamber of spark ignition engine. Sanli et al. 2009 [7] studied by numerical solution the inspection of the impact of engine load and spark timing on the heat transfer of in-cylinder. This study adopted the data of experimental engine (a single cylinder of SI engine four-stroke, air cooled). The Han, Woschni, and Hohenberg models were utilized at (2000 rev/min) with the various engine loads and spark timings. It was noticed that when the spark timing was advanced, the in-cylinder heat flux and heat transfer coefficient increased slightly at constant speed and load. Also, it was seen that when the spark timing was retarded from the original timing, the in-cylinder heat flux and heat transfer coefficient were slightly decreased. On the other hand, the influence of engine load was investigated, and the results showed that the increasing of engine load increases the value of heat flux and heat transfer coefficient. The study also concluded that the higher heat transfer coefficient was obtained from the Han model. Bin Zou et al. 2013 [8] mapping temperature field for exhaust manifold which was taken from CFD and heat process was analyzed for solid domain. The results indicate that the temperature has a major effect on the exhaust manifold mode. Ender et al. 2014 [9] visualized the fluid flow and combustion characteristics of single cylinder SI engine at 1200 rpm. The study was done with a computer simulation, by Star-CD/es-ice. For this simulation, coherent flame model (CFM) was used as combustion model and R-ε-RNG for turbulent model. The pressure, velocity and temperature were plotted during the combustion process. The results showed that, the core temperature was about 2650 K at the center of cylinder when the flame reached. Also, it was noticed that the spark timing has effects on the cylinder pressure, where the pressure is maximum when combustion occurred too early (advanced spark) due to too large work is transfer from the gases to the piston. Vivekanand and Siddaveer 2014 [10] examined the flow through two different models of exhaust manifold to get optimal geometry. The pressure and the velocity contours were drawn for two model and the results showed that the decreasing the back pressure of the exhaust gas is causing increasing the volumetric efficiency of the engine. Naser et al. 2018 [11] used MATHLAB program to evaluate convective heat transfer and the distribution of the radiative heat flux from the gases to the cylinder wall for turbocharged diesel engine type N – 14 at different engine speeds (1200 - 1800 rpm). The study showed that the increase of engine speed is led to increase heat transfer.

This paper represents a modern method in terms of modeling of geometry and 3D simulation by using the finite volume method. The aim of this research is to simulate the flow characteristic and heat transfer in spark ignition engine by using dynamic mesh technique to visualize the flow within engine by using ICE code at different engine speeds. The velocity, pressure, temperature and heat transfer coefficient contours will be investigate with respect to different crank angles and engine speed.

2. Methodology

2.1 CFD Tool

The design and manufacture of internal combustion engines are under significant pressure for improvement. The generation of engines requires being light, reliable, robust, flexible, and powerful. Innovative engine designs will be required for satisfying these requirements. The ability to accurately the performance of multiple engine designs is too much crucial and critical, because IC engines consist of complex fluid dynamic interactions between air flow, fuel injection, moving parts, heat transfer process and combustion. Using CFD results, the flow phenomena can be visualized on a 3D geometry and analyzed numerically, providing tremendous insight into the complex interactions that occur inside the engine. CFD simulation is used as a part of the design process in automotive engineering, especially with the rise of modern technology [4].

2.2 Modeling Geometry

The engine was a four – stroke, spark ignition engine. The combustion chamber is pantroof shape. More information about the engine specification listed in Table (1). The geometric model of engine was created by SolidWorks as shown in figure (1) and (2).

Table (1): Engine Specifications

Bore	71 mm
Stroke	60mm
Connecting rod length	126 mm
Compression ratio	8.2
Intake valve diameter	32 mm
Maximum intake valve lift	6.9 mm at 104 deg. ATDC
Intake valve opening	41 deg. BTDC
Intake valve closing	84 deg. ABDC
Exhaust valve diameter	26mm
Maximum valve lift	9.6 mm at 64 deg. ABDC
Exhaust valve opening	66 deg. BBDC
Exhaust valve closing	16 deg. ATDC

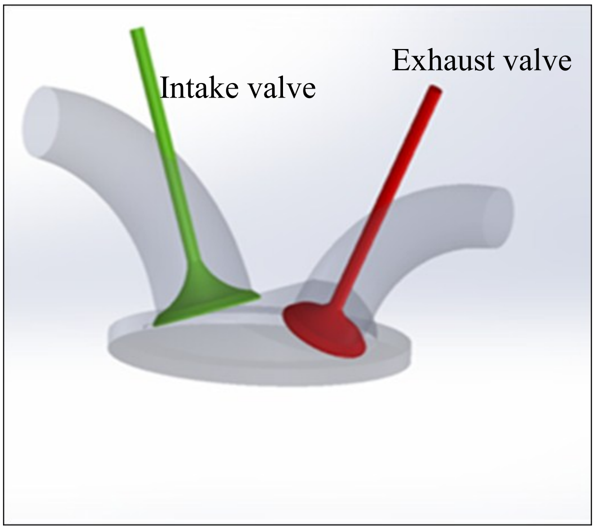

Figure (1): Fluid cylinder model

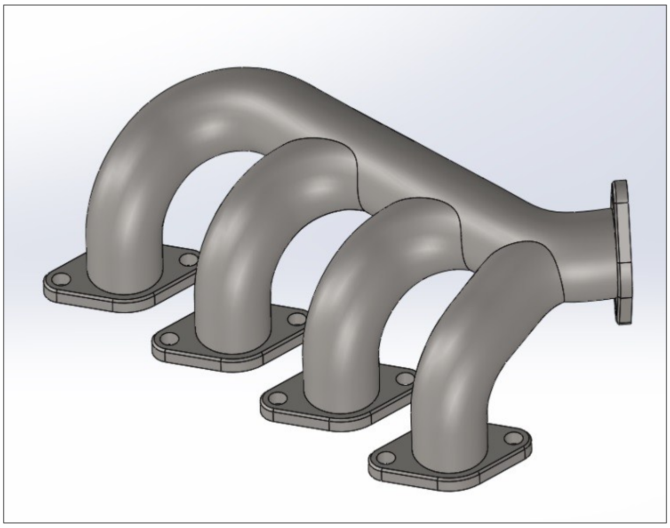

Figure (2): Exhaust manifold model

2.3 Mesh Topology

A Multi zone was taken according to the mechanism of decomposition where, topology (decomposition) is allowing describing the mesh behavior, by dividing the volume of geometry to sub- volumes. Each volume was meshed individually to different elements [12]. In this paper the mesh is deforming (stretches, breaks up, and re-meshes) with respect to time and crank angle (CA). The number of cell is about 407,000. This is acceptable with reasonable limits [6, 13]. The mesh was divided into stationary at intake, exhaust port of engine, moving zone for piston, liner, and combustion chamber regions, as shown in the figure (3). The flow boundary of exhaust manifold is not variable and, the mesh was considering as not variable mesh as shown in the figure (4) and (5).

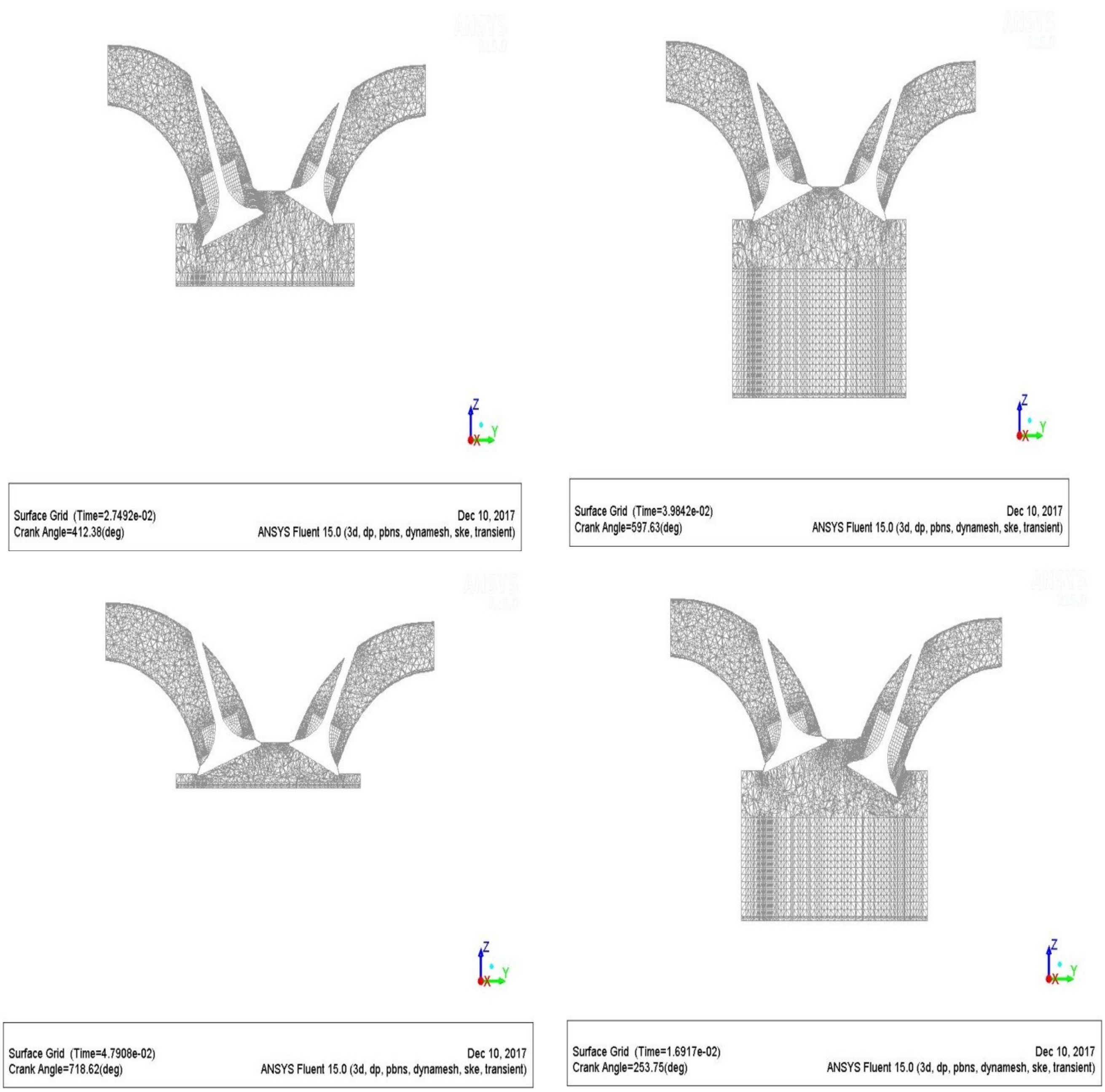

Figure (3): Dynamic mesh of in – cylinder

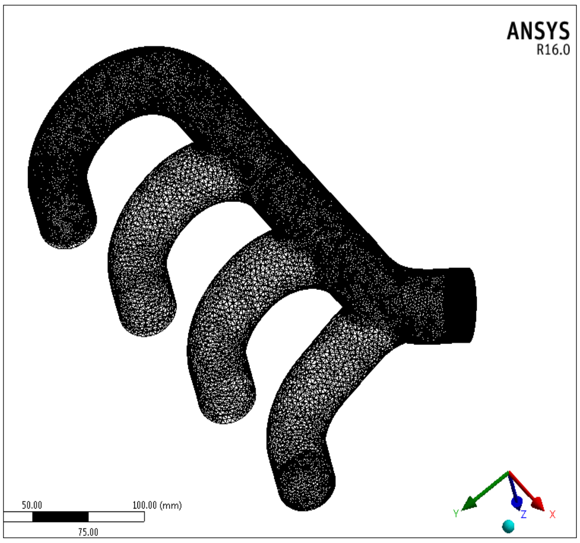

Figure (4): Mesh of fluid domain for exhaust manifold

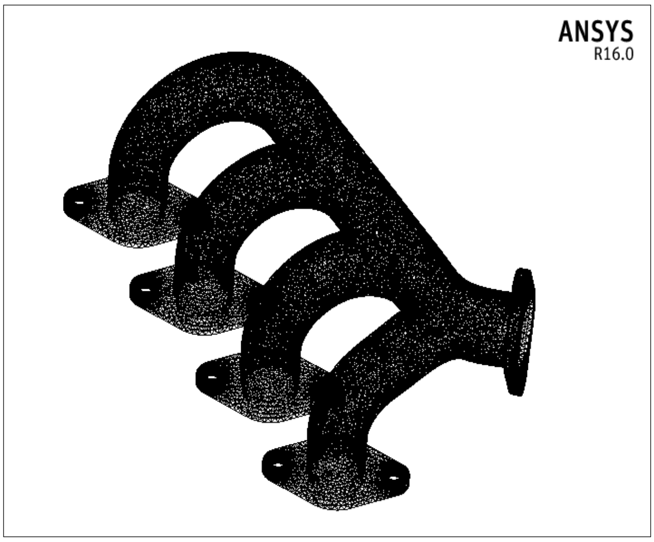

Figure (5): Mesh of solid domain for exhaust manifold

2.4 Motion System

For compatibility between the motion of valves and piston, the motion of these parts was controlled in this simulation. The motion was programmed to describe all events that occurred during the 4-strokes.

To achieve the matching for the moving mesh with piston and valves, the dynamic mesh events are specified according to the valve timing, as shown in equations below and figure (6) [13].

$$\theta_C = \theta_S + t\,\Omega_{shaft} \quad (1)$$

$$\theta_{event} = \theta_c + n\theta_{period} \quad (2)$$

The dynamic mesh model was utilized to model the flow, where the shape of domain is changing with time because of the motion on the domain boundaries. Updating of volume mesh is handled by FLUENT at every time step based on the positions of boundaries, where the events are specified for one complete engine cycle.

$$P_S = L + \frac{A}{2}(1 - COS\theta_C) - \sqrt{L^2 - \frac{A^2}{4}sin^2\theta_c} \quad (3)$$

Where, p_s is equal to zero at TDC and equal A at BDC.

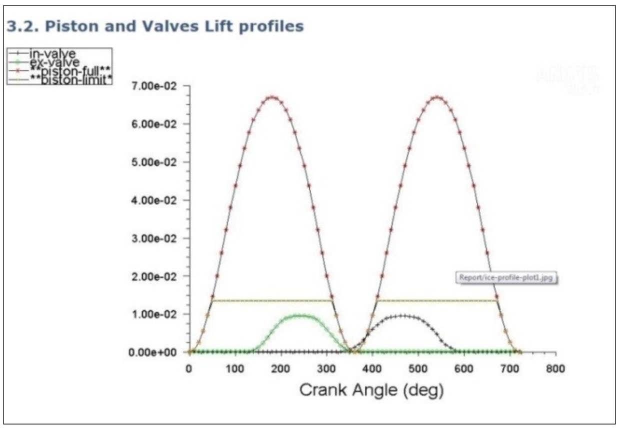

Figure (6): Valves and piston profile

2.5 Governing Equations

The simulation was done under firing condition and included the governing equations of fluid dynamics. These equations are used to characterize the mass, momentum, energy, k-ε turbulence, unsteady (transient) model, without spray and chemical reactions, are given as follows [14]:

- **Continuity Equation**

The conservation of mass can be written as a mass balance for the fluid, where the mass enters a system is equal to the rate at which mass leaves the system.

$$\frac{\partial \rho}{\partial t} + div.(\rho u) = 0 \qquad (4)$$

- **Momentum Equation**

The first term represents the time rate of change of the momentum into volume element, the second term is the change due to pressure force, the third term is the rate of change due to viscous forces, and the fourth term is body forces.

$$\rho \frac{Du}{DT} = -\frac{\partial p}{\partial x} + \frac{\partial \tau_{xx}}{\partial x} + \frac{\partial \tau_{yx}}{\partial y} + \frac{\partial \tau_{zx}}{\partial z} + S_{Mx} \qquad (5)$$

- **Energy Equation**

The rate of increase of energy of fluid particle is equal to the net rate of added to fluid particle.

$$\rho \left[\frac{\partial h}{\partial t} + div.(hV)\right] = -\frac{Dp}{Dt} + div(kgrdT) + \varphi \qquad (6)$$

- **Turbulent Model**

The k-ε model is the simplest of turbulence consisting of two equations model. It is a semi-empirical model, and the derivation of the model eqn. Relies on phenomenological considerations and empiricism [15]. Turbulent is more important in internal combustion engine, so the k- ε taken to specifies it. Two equations of k and ε [13] allow to calculations of both, time scale and turbulent length. It represents the robustness, and reasonable accuracy for more range of turbulent flow. The following equations were used to achieve compression ratio which is required in the engine that used in this work.

$$\frac{\partial}{\partial t}(\rho k) + \frac{\partial}{\partial x_i}(\rho k u_i) = \frac{\partial}{\partial x_j}\left[\left(\mu + \frac{\mu_t}{\sigma_k}\right)\frac{\partial K}{\partial x_j}\right] + G_k + G_b - \rho\varepsilon - Y_M + S_K \qquad (7)$$

$$\frac{\partial}{\partial t}(\rho \varepsilon) + \frac{\partial}{\partial x_i}(\rho \varepsilon u_i) = \frac{\partial}{\partial x_j}\left[\left(\mu + \frac{\mu_t}{\sigma_\varepsilon}\right)\frac{\partial \varepsilon}{\partial x_j}\right] + C1_\varepsilon \frac{\varepsilon}{K}\left(G_k + C_{3\varepsilon} G_b\right) - C_{2\varepsilon}\rho \frac{\varepsilon^2}{k} + S_\varepsilon \qquad (8)$$

$$\mu_t = \rho C_\mu \frac{k^2}{\varepsilon} \qquad (9)$$

Where: $C_{1\varepsilon} = 1.44$, $C_{2\varepsilon} = 1.92$, $C_\mu = 0.09$, $\sigma_K = 1.0$, and $\sigma_\varepsilon = 1.3$

2.6 Boundary Conditions

The flow domain for this simulation is the combustion chamber, including the inlet valve, exhaust valve, piston , also intake and exhaust port . The boundary conditions have been used refers to the pressure inlet boundary conditions , the pressure outlet boundary condition for the exit from the exhaust port. The intial condition are given in Table (2) and, the results of the exhaust port for crank angles are used as an input data for the exhaust manifold. The firing order are considered at (runner 1,4 are open) and, (runner 2,3 are open). The material of exhaust manifold is aluminum.

Table (2): Boundary and initial conditions

Variable (unit)	Initial value
Pressure (Pa)	Atmospheric pressure
Turbulent kinetic energy (m^2/s^2)	0.02
Turbulent dissipation rate (m^2/s^3)	0.02
Temperature (k)	300
Inlet pressure (Pa)	Atmospheric pressure
Exhaust pressure (Pa)	Atmospheric pressure
Cylinder wall temperature (k)	300
Piston wall temperature (k)	300

3. Results and discussions

Various numerical analyses were achieved to estimate the flow characteristics and heat transfer for the 4- strokes of the reciprocating engine. The results of the distribution of in – cylinder pressure at different engine speeds for various crank angles are given in figures (7and 8). The results show that the pressure vacuum at intake stroke because the intake valve starts open at 360 degree, the piston moves from TDC toward down so the volume of combustion chamber is increased, and then pressure reduced. Then when the piston moves up from BDC to TDC, the volume is decreased so the pressure increased, and then gradually increasing at the 2nd stroke. According to the valve timing, the fuel injection at the end of 2nd stroke, into chamber, prepares the mixture for ignition by spark. Then combustion occurs and the results shown in figure (8) reveal that the pressure increases at 720 CA. And, it reduces gradually due to the conversion the fuel power to mechanical power at power stroke. During the exhaust stroke, the code shows a decrease in the value of pressure according to the expanding at the end of the third stroke because piston moves towards the BDC, the flow blow down exhaust system. Also the results show the pressure is increases with increasing of engine speed.

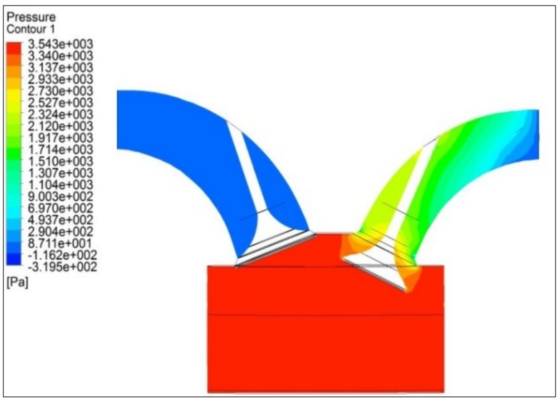

1500 engine speed

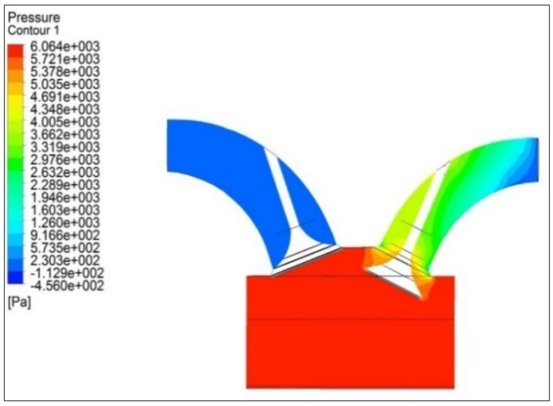

2000 engine speed

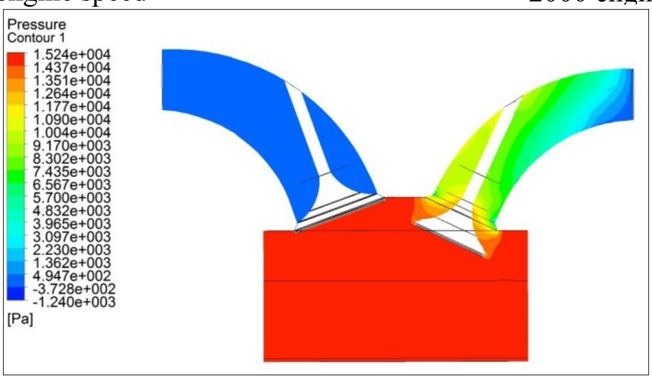

Figure (7): The pressure contours at 990 crank angle for different engine speeds

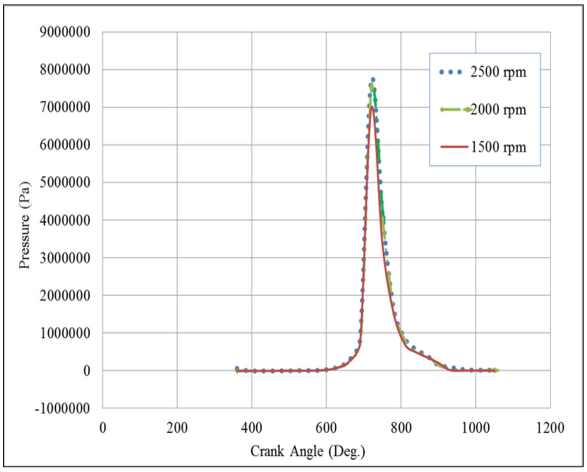

Figure (8): The in –cylinder pressure distribution for different engine

Figure (9and 10) show the temperature distribution for different engine speeds. It's obvious that the speed of engine is effects on the temperature where, the temperature increases with increasing engine speed due to the turbulence increasing and, the maximum value during the flame propagation at 2500 rpm. The temperature distribution in the combustion chamber is given against crank angles as shown in figure (10).

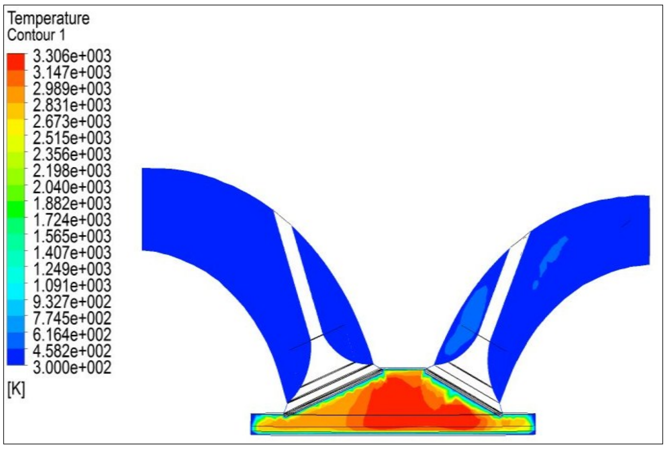

1500 engine speed

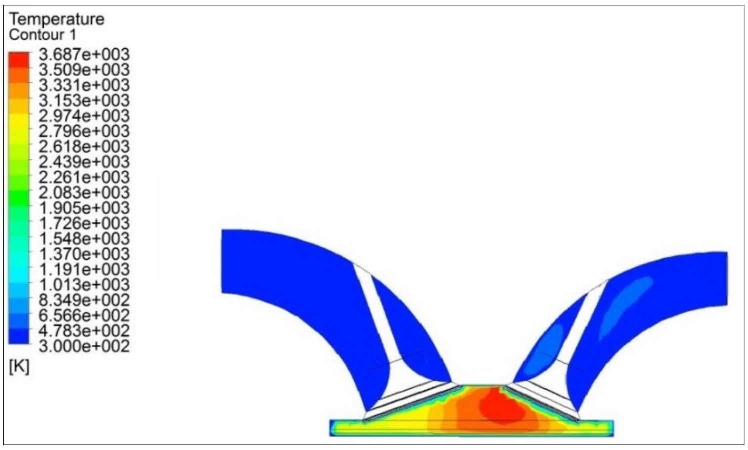

2000 engine speed

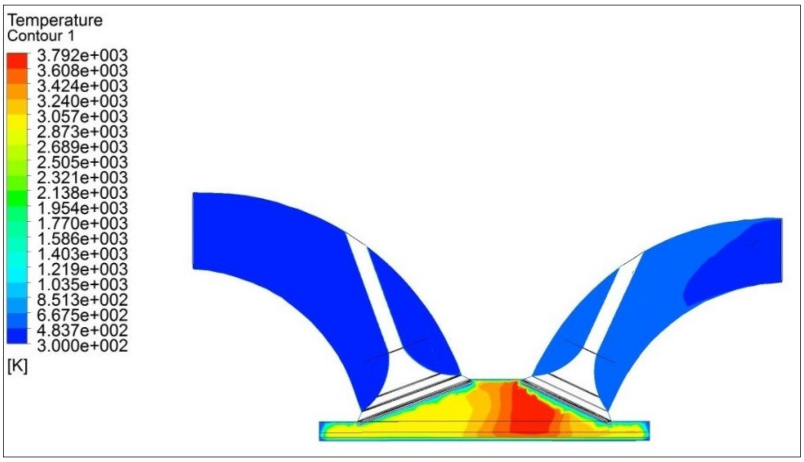

2500 engine speed

Figure (9): The temperature contours at 720 crank angle for different engine

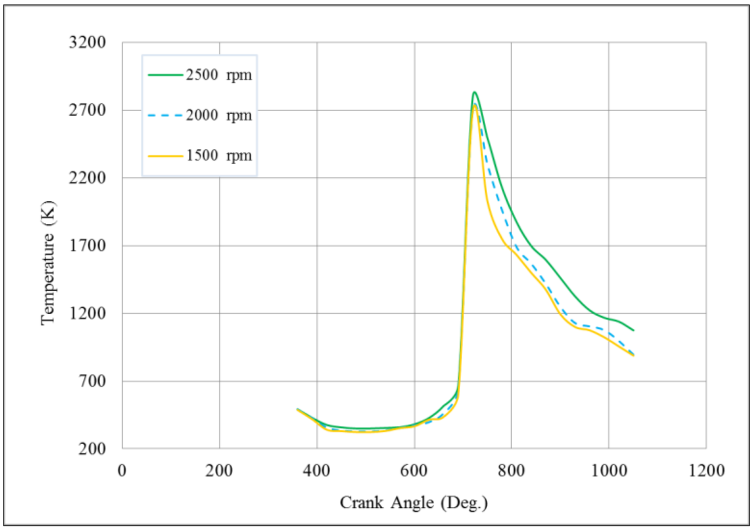

Figure (10): The temperature distribution in the combustion chamber at different engine speeds

Also from CFD analysis, velocity inside the exhaust port for 1500 and 2500 rpm are shows in the figure (11). Beside that the heat transfer coefficient inside combustion chamber, piston, intake and exhaust port were also estimated during four – strokes and the distribution were drawn in the figures (12-14) respectively. From the results in this work conclude that when the engine speed increases, the velocity of gases of engine will increase and this causes to a rise in convective heat transfer coefficient. As a result, the heat transfer increases. From figure (12 and 13) it is seen that during the combustion, the heat transfer coefficient is increases. It is the maximum value at 720 CA. Moreover, it noted that the value of HTC of combustion chamber is high more than piston, intake and exhaust port of combustion engine at the same rpm. Figure (14) exhibit that the heat transfer coefficient of intake port is extremely a high value at 1st stroke due to the interaction between the gas in the intake port wall and the engine cylinder. In the 2nd, 3rd and 4th stroke, the intake valve is closed, therefore the heat from combustion process in engine cylinder is not interacting with the intake port wall, where the flow of hot gases does not reach the port wall. In this circumstance, the turbulence intensity of gas flow velocity increases in the intake port with increasing of engine speed as shown in figure (15) and this led to increase the value of the heat transfer coefficient. This fact agrees with [16] and [17]. Figure (16) illustrates the heat transfer behavior in the exhaust port of IC engine at different engine speeds. It is seen that the HTC is high at 2500 rpm due to the increase of turbulent, velocity of flow gases, and this matches with increasing HTC of combustion chamber at the same rpm.

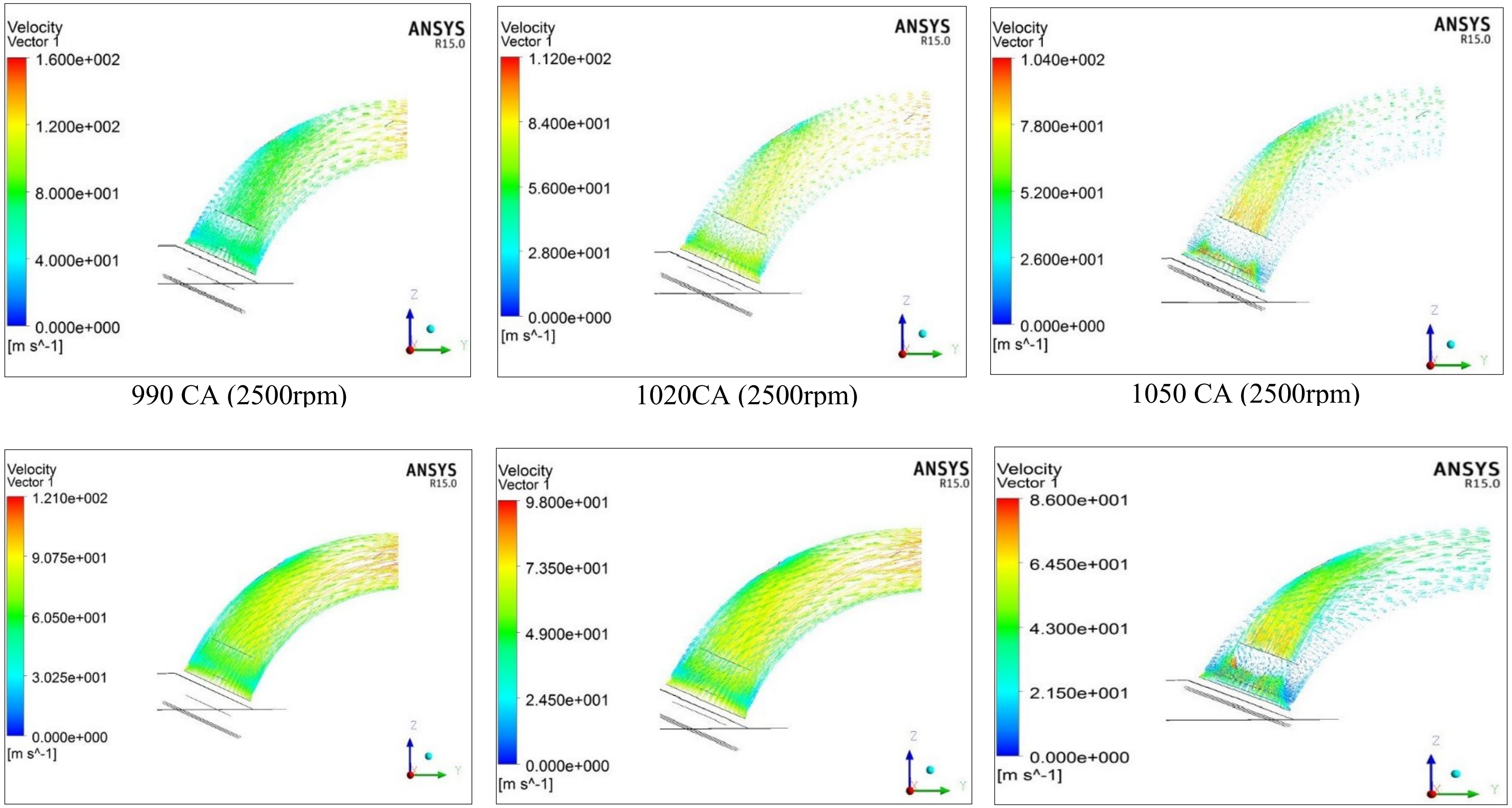

990 CA (2500rpm) | 1020CA (2500rpm) | 1050 CA (2500rpm)

990 CA (1500rpm) | 1020CA (1500rpm) | 1050 CA (1500rpm)

Figure (11): The velocity contours in the exhaust port at different engine speeds (1500, 2500 rpm)

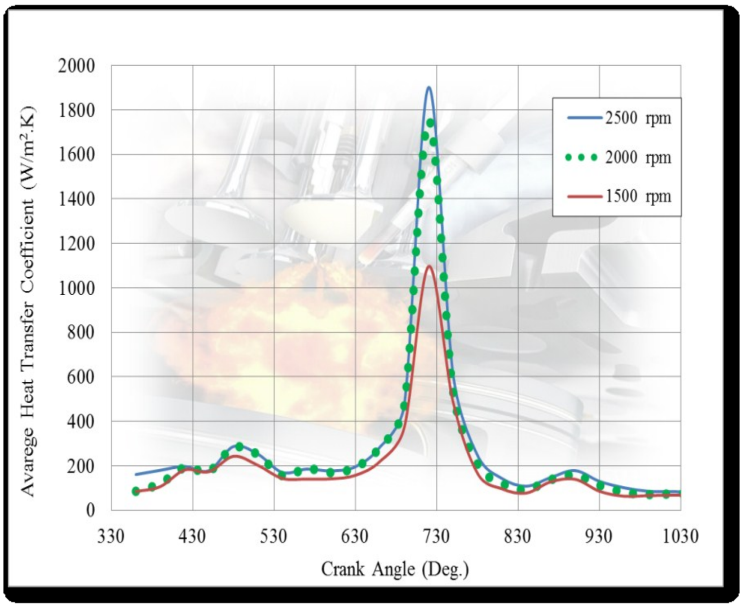

Figure (12): Average convective heat transfer coefficient within combustion chamber at different engine speeds

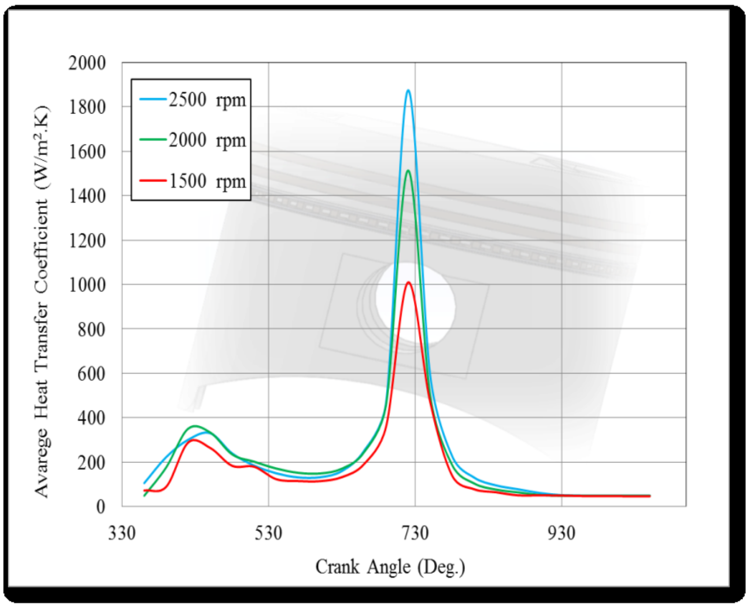

Figure (13): Average convective heat transfer coefficient on crown piston at different engine speeds

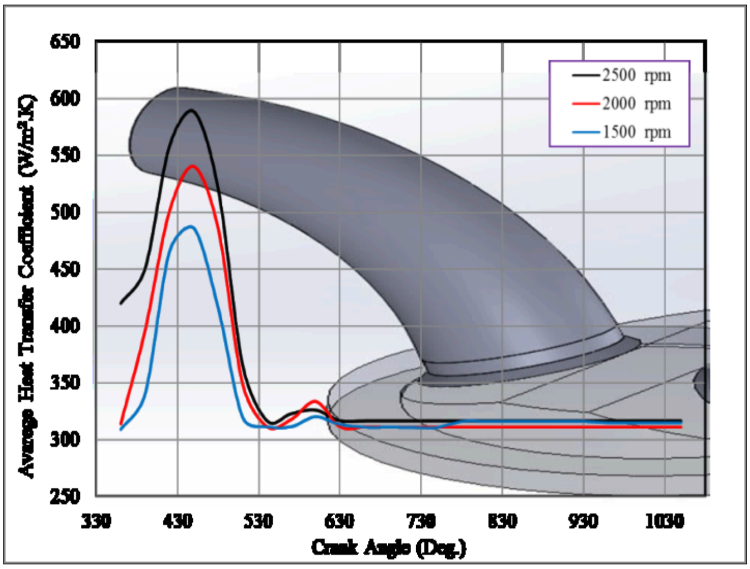

Figure (14): Average convective heat transfer coefficient for intake port different engine speeds

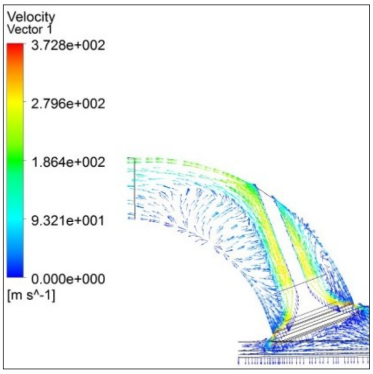

Engine speed 2500
CA: 360 Degree

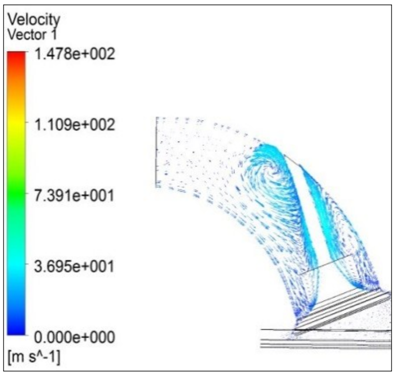

Engine speed 1500
CA: 360 Degree

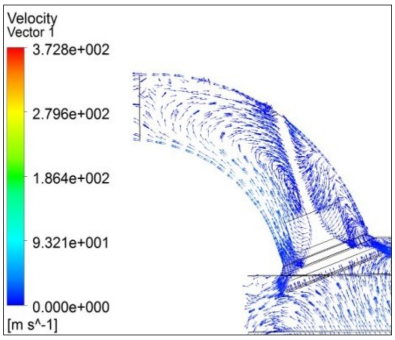

Engine speed 2500
CA: 540 Degree

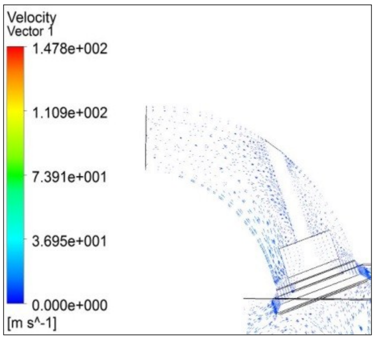

Engine speed 1500
CA: 540 Degree

Figure (15): Velocity contours for intake port at 1500 and 2500 rpm during intake stroke

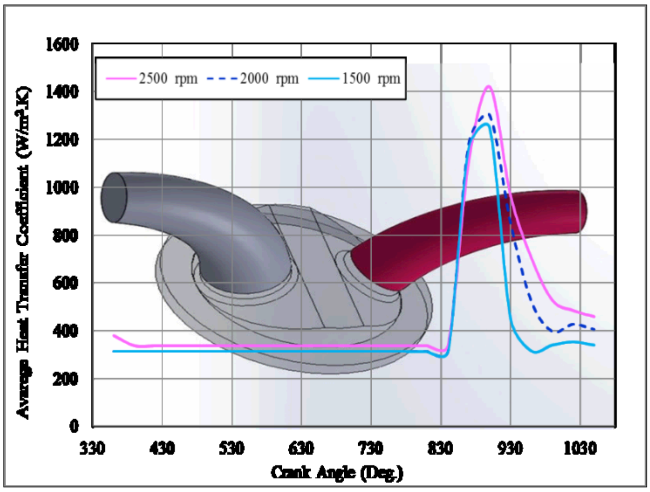

Figure (16): Average convective heat transfer coefficient for exhaust port at different engine speeds

The pressure and temperature in the engine at 2500 rpm are higher than (1500 and 2000 rpm). And therefore, this work discuss the behavior of flow using finite volume method (FVM) and solid domain by utilizing finite element method (FEM) for the exhaust manifold at 2500 rpm. The pressure contours for different crank angles are given in the figures (17, 18 and 19). It can be seen that the pressure is decreased throughout the exhaust manifold and, it's clearly drop at the region of the exhaust manifolds outlet's.

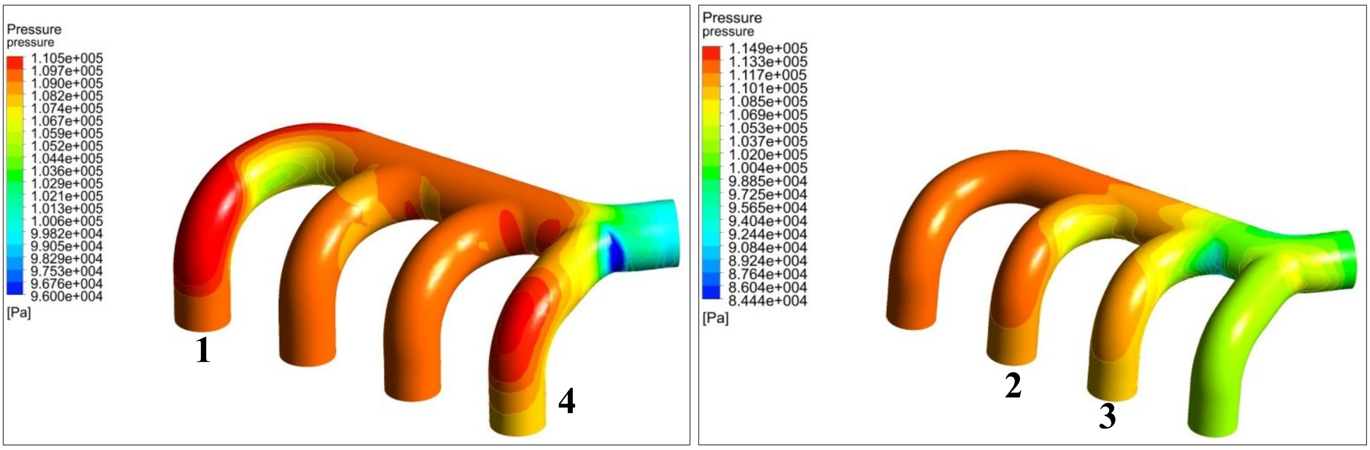

Runner 1 and 4 are

Runner 2 and 3 are

Figure (17): Pressure distribution for flow of exhaust manifold at 990

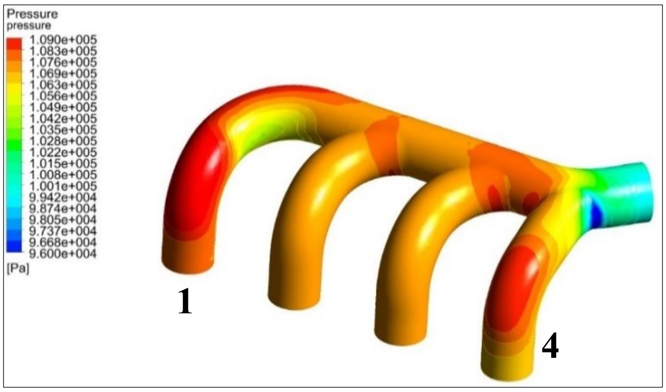

Figure (18): Pressure distribution for flow of exhaust manifold at 1020 CA

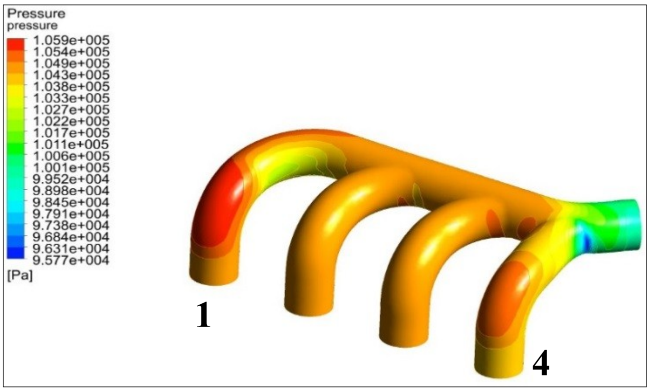

Figure (19): Pressure distribution for flow of exhaust manifold at 1050 CA

The temperature is high at the open runners and is fluctuated in the outlet region as compared to other regions as shown in the figures (20-25). It can be noticed that the temperature distribution at the outlet is less when the runners (2&3 are open).

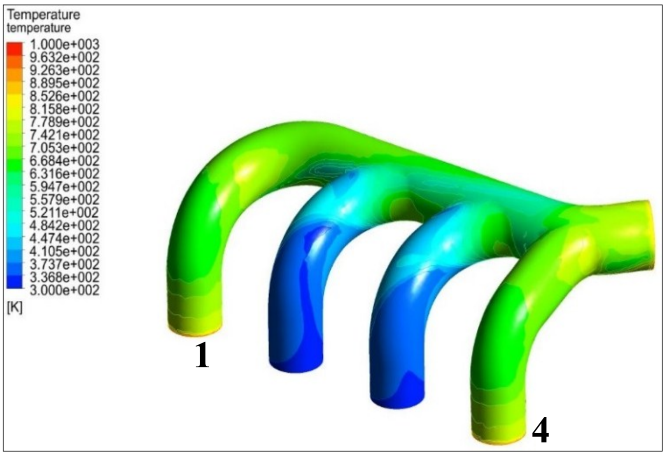

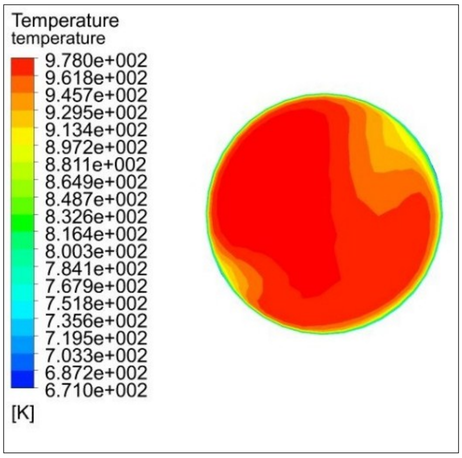

Runner 1 and 4 are open

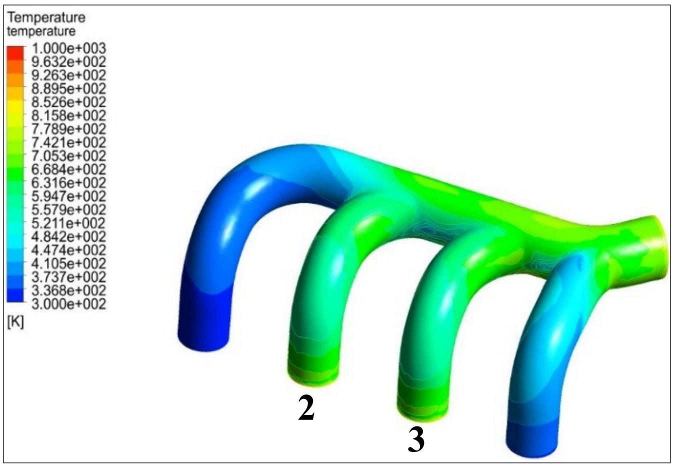

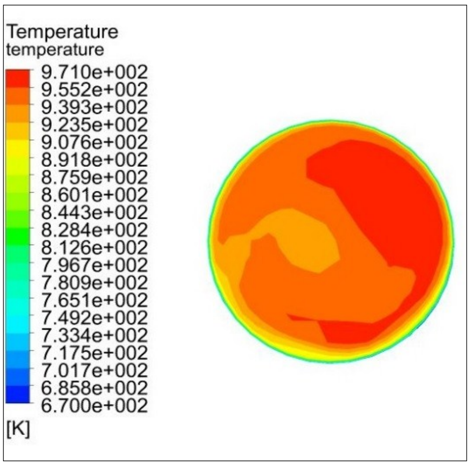

Runner 2 and 3 are open

Figure (20): Temperature distribution for flow of exhaust manifold at 990 CA

Figure (21): Temperature distribution for outlet flow of exhaust manifold at 990 CA

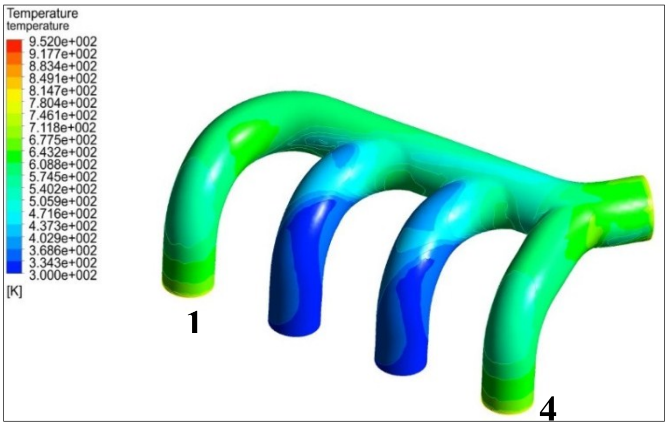

Figure (22): Temperature distribution for flow of exhaust manifold at 1020

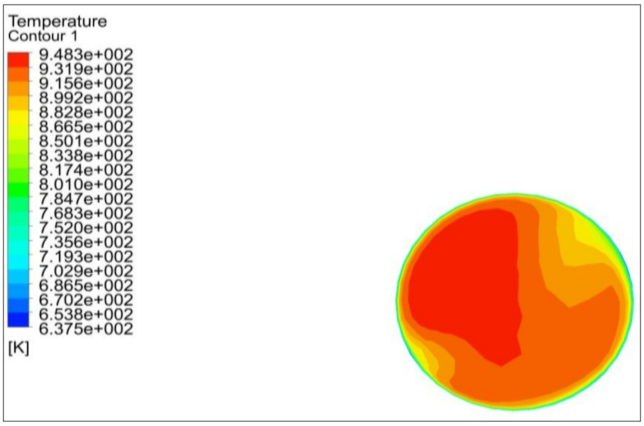

Figure (23): Temperature distribution for outlet flow of exhaust manifold at 1020

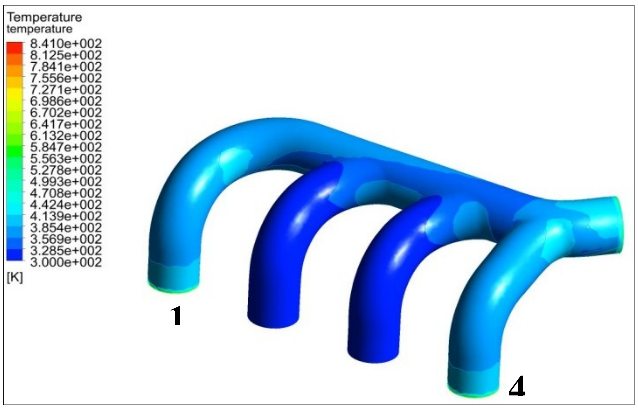

Figure (24): Temperature distribution for flow of exhaust manifold at 1050 CA

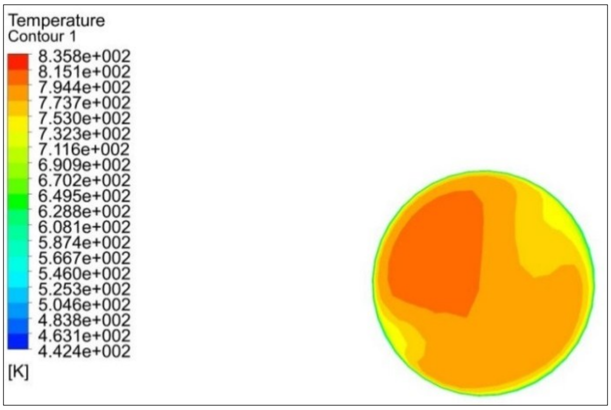

Figure (25): Temperature distribution for outlet flow of exhaust manifold at 1050 CA

From the velocity contours it can be noticed that the maximum value of gases velocity is achieved nearby the outlet of the exhaust manifold because at this position the value of back pressure is low and this agree with [18 and19]. Figures (26-31) refer to the velocity vector and contours of the outlet velocity respectively during exhaust stroke. Also heat transfer coefficient for the exhaust manifold was studied and shows that the heat transfer is function for velocity parameter. The convective heat transfer coefficient is high at the bend pipe and the maximum value is achieved at the outlet due to high value of velocity where the gases combined from four ports of manifold and leave from the outlet.

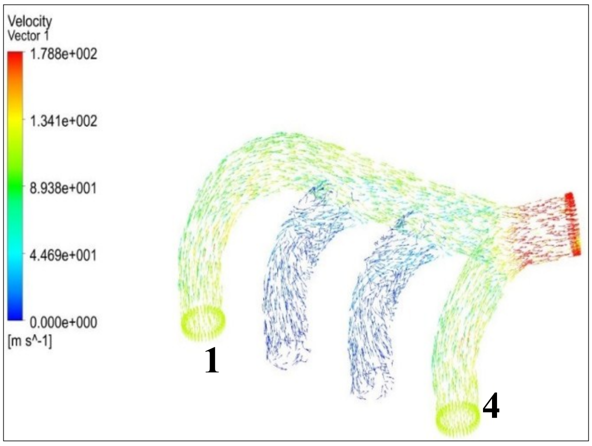

Runner 1 and 4 are

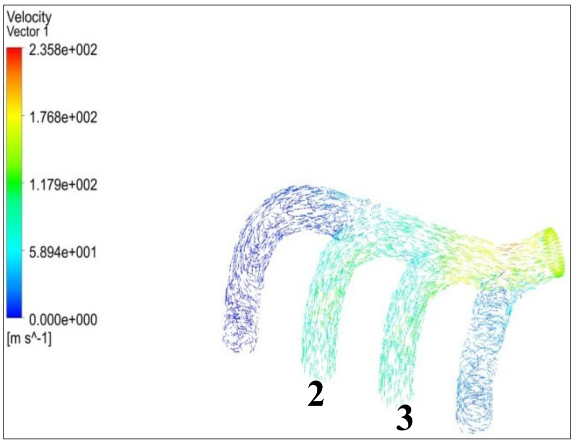

Runner 2 and 3

Figure (26): Velocity distribution for flow of exhaust

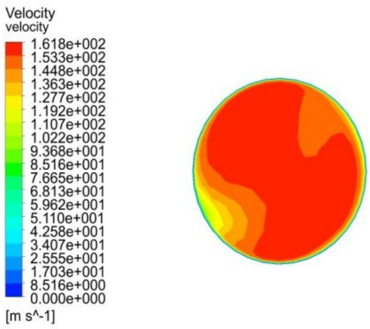

Figure (27): Velocity distribution for outlet flow of exhaust manifold at 990 CA at runner 1 and 4 are open

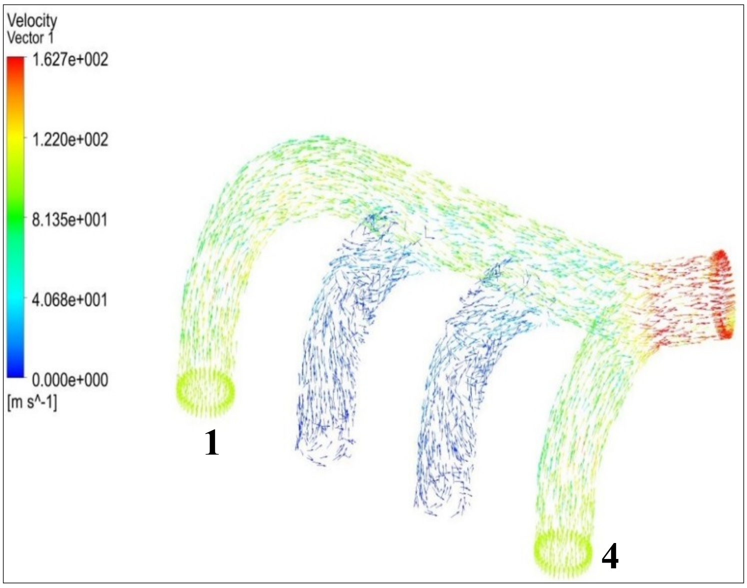

Figure (28): Velocity distribution for flow of exhaust manifold at 1020 CA

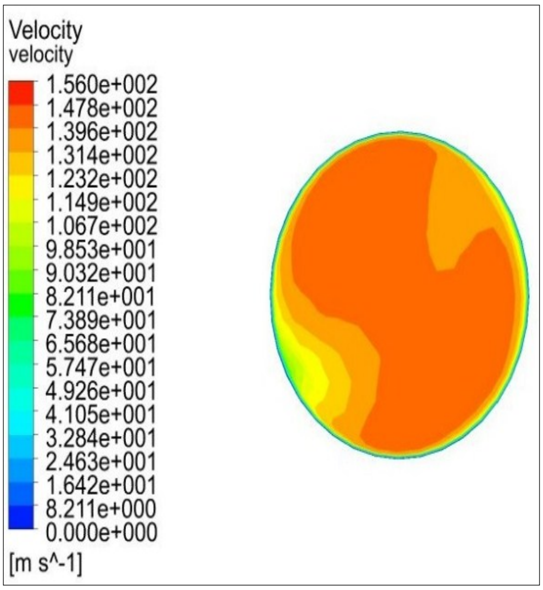

Figure (29): Velocity distribution for outlet flow of exhaust manifold at 1020

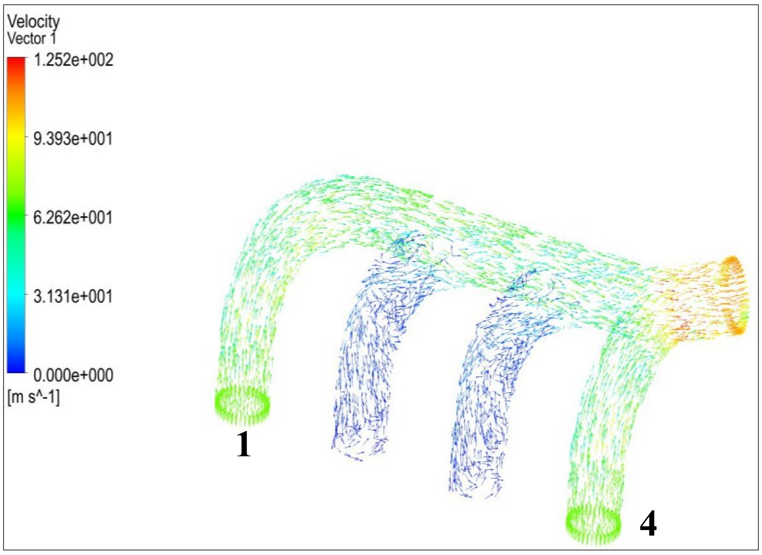

Figure (30): Velocity distribution for flow of exhaust manifold at 1050 CA

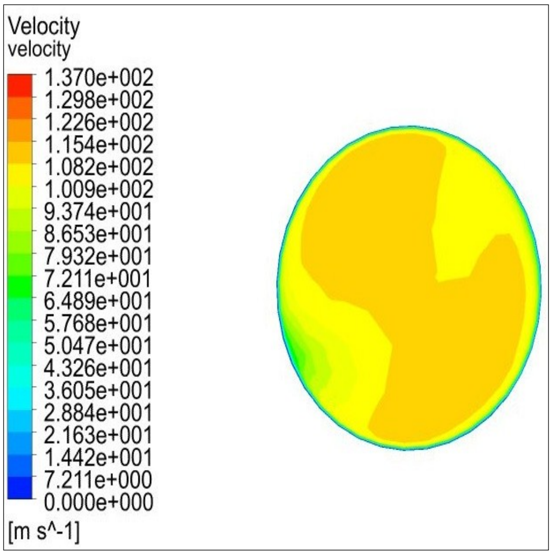

Figure (31): Velocity distribution for outlet flow of exhaust manifold at 1050

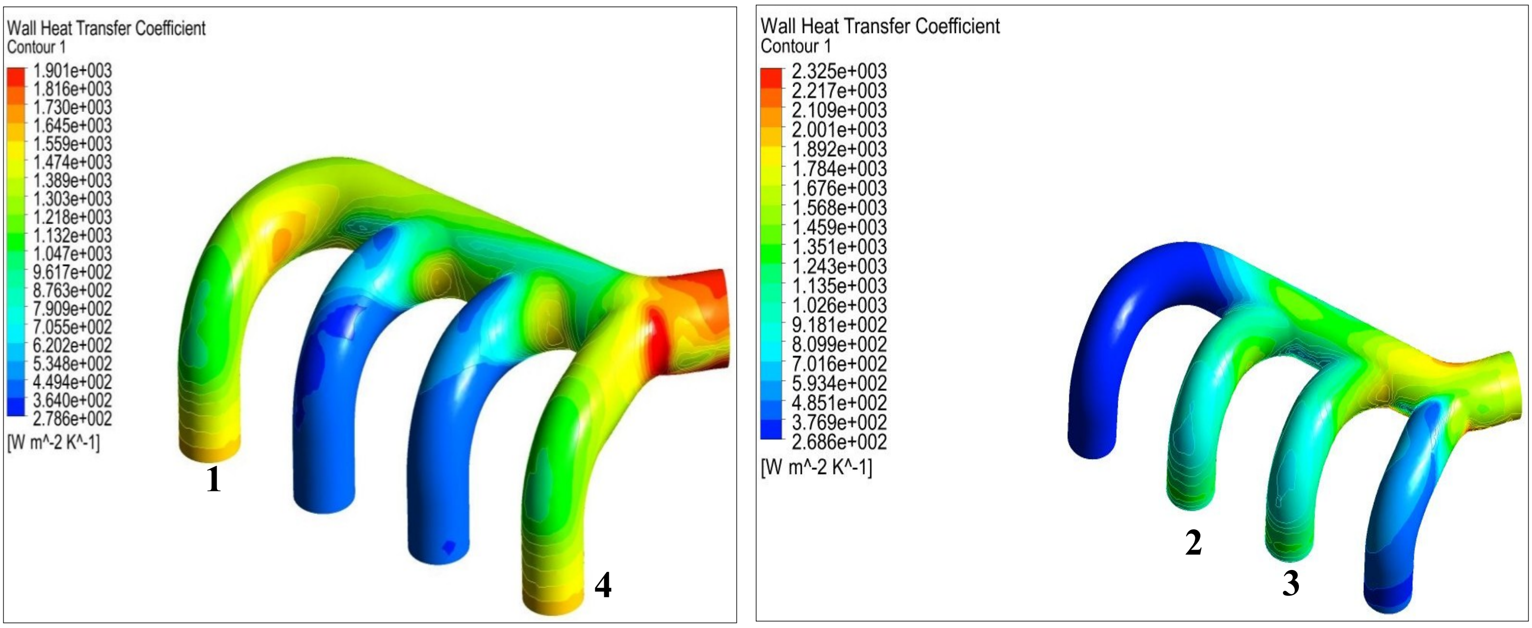

Runner 1 and 4 are open

Runner 2 and 3 are open

Figure (32): Average convective heat transfer coefficient at 990 CA

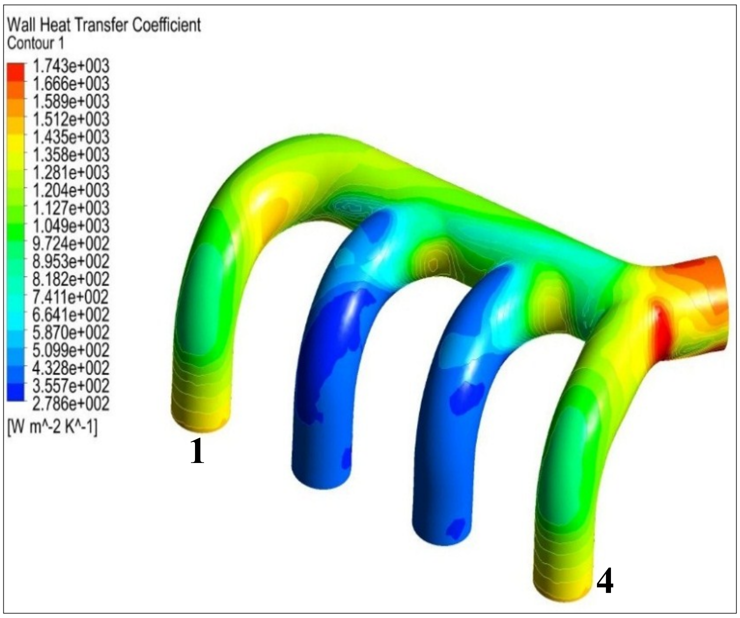

Figure (33): Average convective heat transfer coefficient at 1020 CA

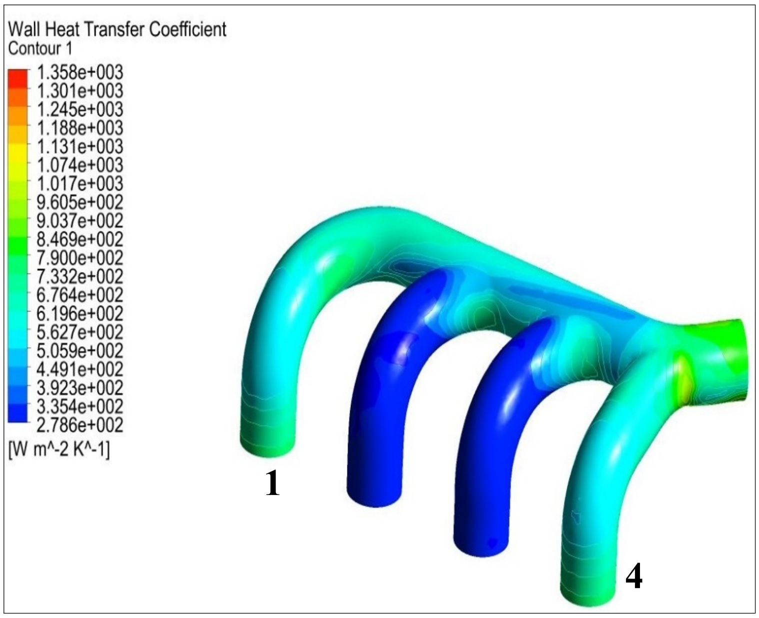

Figure (34): Average convective heat transfer coefficient at 1050 CA

The rises of temperature occur at the points of gases mixing, because of the friction and collision between the molecules of gases as shown in figure (35).

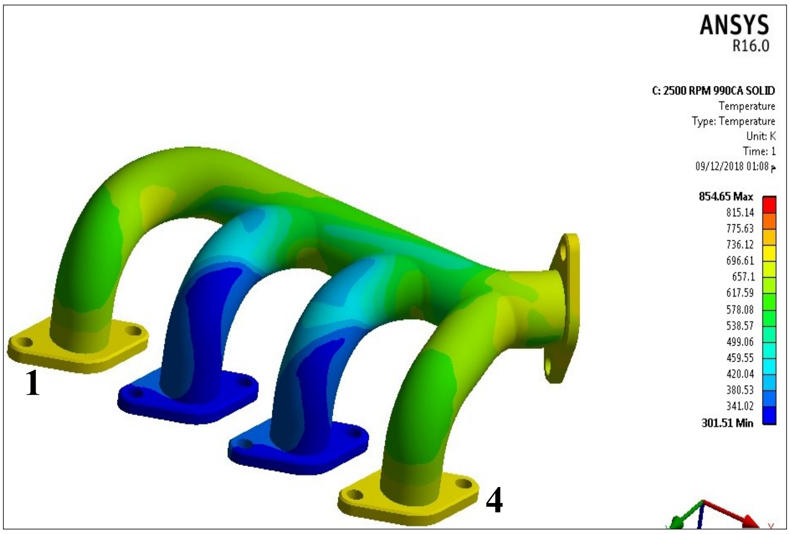

990 CA Runner 1 and 4 are open

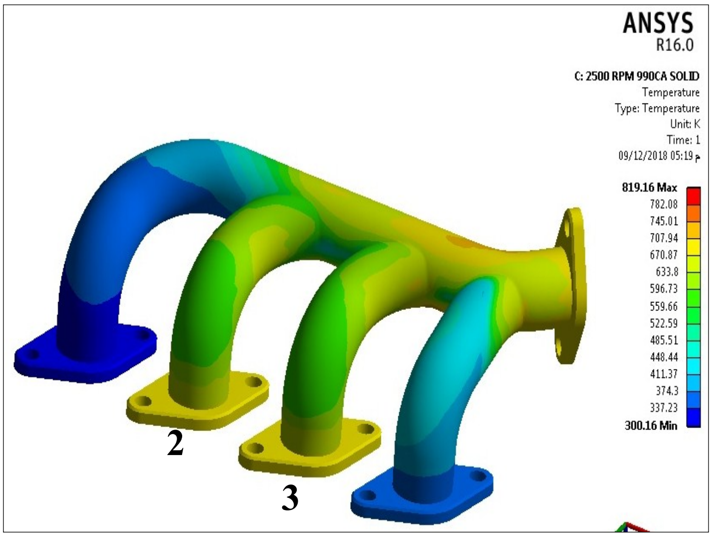

990 CA Runner 2 and 3 are open

1020 CA

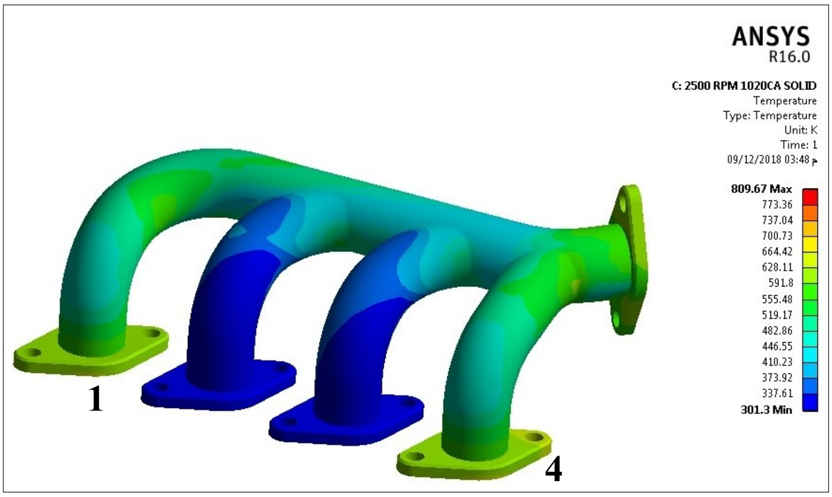

1050 CA

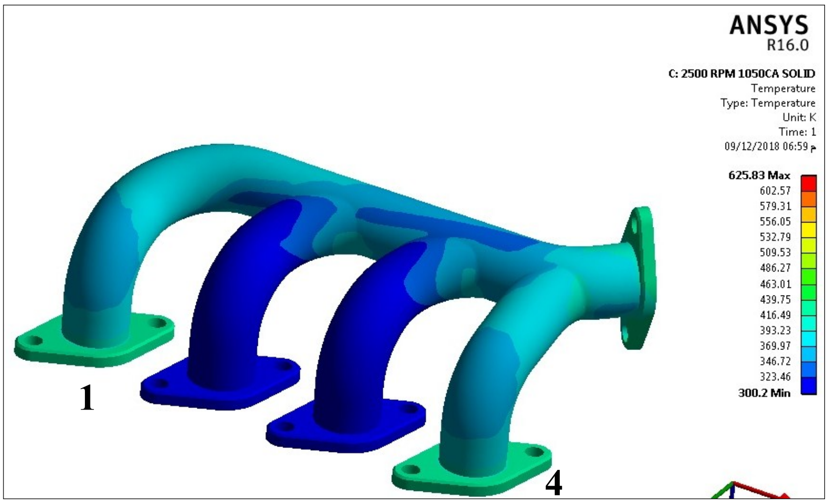

Figure (35): Temperature distribution of solid domain of exhaust manifold at different crank angle

4. Validation

The validity of this paper has been examined by comparing the results with other published researches as show below.

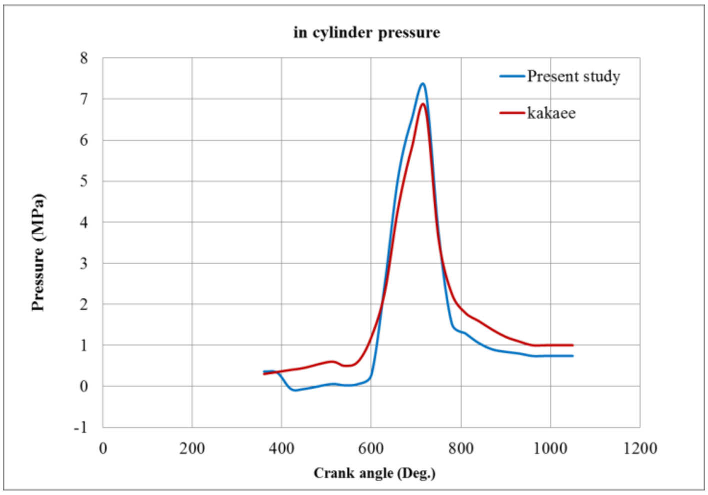

Figure (36): Comparession between in– cylinder pressure with the publishers [20].

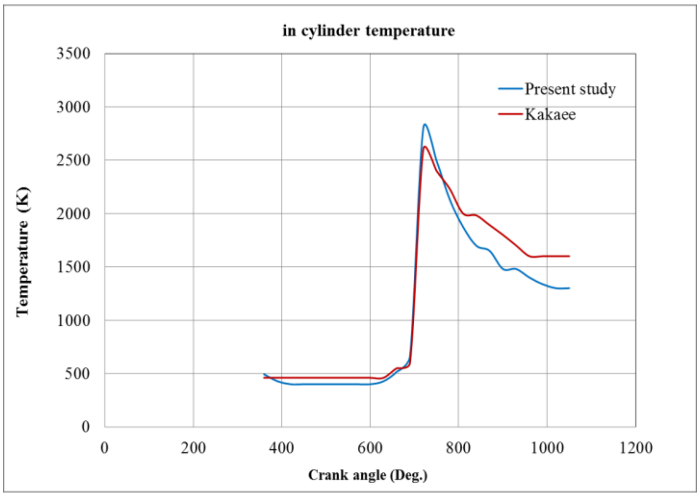

Figure (37): Comparession between in – cylinder temperature with the publishers [20].

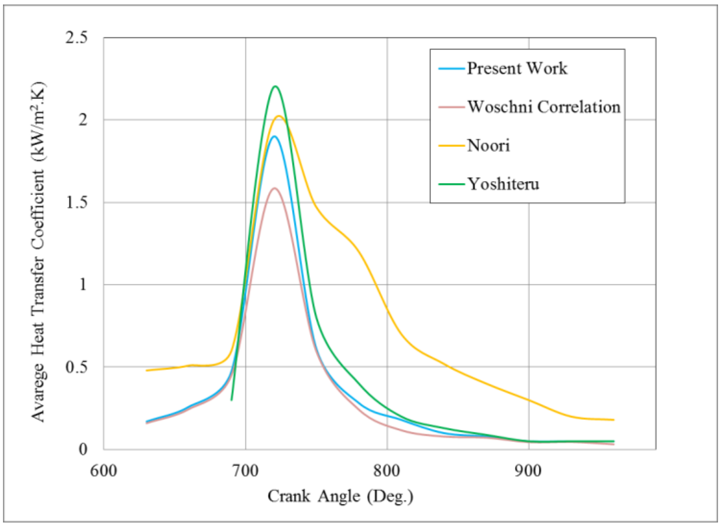

Figure (38): Comparession between HTC (CFD) in combustion chamber with the publishers [21, 22, and 23].

5. Conclusions

The flow characteristics within SI engine were investigated utilizing CFD ICE CODE. The temperature, pressure, and velocity were plotted with respect to the crank angle for different engine speeds. As a result, the following conclusions were summarized:

- The adopted approach of the modeling of combustion simulation via ANSYS ICE CODE with dynamic mesh technique can be used to develop of internal combustion engine.
- The value of temperature and pressure for firing simulation were bit higher than researches experimental due the fact this simplified CFD simulation doesn't include friction losses induced interactions of engine components.
- Flow characteristic (Pressure, Velocity and Temperature) increasing with increasing of engine speed (rpm). And, there is a relationship between heat transfer coefficients and above characteristic, the heat transfer coefficient increases with increasing rpm.
- The maximum value of heat transfer coefficient is achieved at the outlet of the exhaust manifold when the value of engine speed is increase.

References

[1] James P. Myers, Alexandros, "Effects of Combustion-Chamber Surface Temperature on the Exhaust Emissions of a Single-Cylinder Spark-Ignition Engine," SAE Technical Paper,1978.

[2] A.C. Alkidas, J.P. Myers, "Transient Heat Flux Measurements in the combustion chamber of a spark ignition engine", ASMEJ. Heat Transfer 104 (1982) 62-67.

[3] Heywood, JB. "Internal Combustion Engine Fundamentals". New York, NY, McGraw Book Company, 1988.

[4] Y. Harigaya, F. Toda, M. Suzuki, "Local Heat Transfer on Combustion Chamber Wall of a Spark Ignition Engine", SAE Paper No.931130, 1993, PP.1567-1575.

[5] Kleemann, A.P, Gomsan, A.D., and Binder, K.B., "Heat Transfer in Diesel Engines: A CFD Evaluation Study", the 5th international COMODIA Symposium on Diagnostic and Modeling of Internal Combustion Engine, 2001.

[6] A. Mohammadi, A. Jazayeri, M. Zbashrahagh. N., "Numerical Simulation of Convective Heat Transfer in a Spark Ignition Engine" ICE Division of ASME, Spring Technical Conference, Chicago, Illinio, USA, 2008.

[7] A. Sanli, C. Sayin, M. Gumus ,I.Kilicaslan, and M.Canakci " Numerical Evaluation by Models of Load and Spark Timing Effect on the In-Cylinder Heat Transfer of A SI Engine" Numerical Heat Transfer,Vol.56,pp:444-458, 2009.

[8] Ben Zou, Yaqian Hu, Zhien Lin, Fuwn Yan and ChaoWong, "The Impact of The Temperature Effect on Exhaust Manifold Thermal Model Analysis" Research Journal of Applied Sciences Engineering and Technology, August, 2013, PP 2824-2829.

[9] Ender Hepkaya,Salih Karaaslan,Sitki Uslu,Nureddin Dinler and Nuri Yucel, "A Case Study of Combustion Modeling in a Spark Ignition Engine Using Coherent Flame Model", Journal of Thermal Science and Technology,2014, ISSN 1300-3615.

[10] Vivekanand Navadagi, Siddaveersanganad "CFD Analysis of Exhaust Manifold of Multi Cylinder Petrol Engine for Optimal Geometry to Reduce Back Pressure", International journal of engineering Research and Technology (IJERT) 2014.

[11] Naser LAJQI, Azem KYÇYKU, Shpetim LAJQI, "Modeling and Simulation of Heat Transfer in Turbocharged Diesel Engines", International Journal of Mechanical Engineering and Technology (IJMET) Volume 9, Issue 1, January 2018, pp. 308–319.

[12] ANSYS Version 15.0 Help Library.

[13] Kurniawan W.H, Abdullah S, and Shamsudeen, "Turbulence and Heat Transfer Analysis of Intake and Compression Stroke in Automotive 4-stroke Direct Injection Engine", Algerian Journal of Applied Fluid Mechanics, Vol. 1, 2007.

[14] K. M. Ravichandra, D. Manikanta, M. Kotresh, “CFD Simulation of an IC Engine by Producer Gas” International Journal of Civil Engineering and Technology (IJCIET) Volume 8, Issue 10, October 2017, pp. 145–152.
[15] B.E.Londer and D.B. Spalding “Lectures in Mathematical Models of Turbulence “Academic press, London, 1972.
[16] Semien, Abdul Rahim Ismail, Rosli Abu Bakar and Ismail Ali, “Heat Transfer of Intake Port Based on Steady –Steady-State and Transient Simulation”,Sciences,2008 PP:1572-1579.
[17] Simeon, “Heat Transfer Investigation in the Intake Port of 4 Stroke Direct Injection Compression Ignition Engine”, ACTA TECHNICA CORVINESIS, 2013, ISSN 2067-3809.
[18] C. Krishnara J1, S Rajesh Ruban, N. Subramani, “Analysis of Exhaust Manifold to Improve the Engine Performance”, International Journal of Engineering & Technology, 7 (2.8) (2018) 539-542.
[19] Sagar G. Rautrao, Bhagwan R. Shinde, “ Numerical Study of Exhaust Manifold using Conjugate Heat Transfer”, International Journal of Engineering and Advanced Technology (IJEAT) ISSN: 2249 – 8958, Volume-6 Issue-5, June 2017.
[20] Kakaee, Gharloghi, Foroughfar, and Khanlari. “Thermo-Mechanical Analysis of an SI Engine Piston Using Different Boundary Condition Treatments”, J. Cent. South Univ. (2015) 22: 3817−3829 DOI: 10.1007/s11771-015-2926-7 Springer.
[21] G. Woschni, “A Universal Applicable Equation for the Instantaneous Heat Transfer Coefficient in the Internal Combustion Engine: , SAE Paper,No.670913,1963.
[22] A. R. Noori and M. Rashidi, “Computational Fluid Dynamics Study of Heat Transfer in a SI engine Combustion Chamber”, ASME,Vol. 129, 2007.
[23] Yoshiteru ENOMOTO and Shoichi FURUHAMA, “ A Study of the Local Heat Transfer Coefficient on the Combustion Chamber Walls of a Four-Stroke Gasoline Engine” , JSME, International Journal, Series II,Vol.32,No.1,pp:107-114,1989.